# Novel mixed H+/e-/O2- conducting cathode material PrBa0.9K0.1Fe1.9Zn0.1O5+δ for proton-conducting solid oxide fuel cells

Bo Liu [a], Zongbao Li [b], Xinwei Yang [a], Dong Yan [a], Jian Li [a], Lichao Jia [a*]

[a] *School of Materials Science and Engineering, State Key Lab of Material Processing and Die & Mould Technology, Huazhong University of Science and Technology, Wuhan 430074, China. E-mail: jialc@hust.edu.cn*

[b] *School of Materials Science and Engineering, Wuhan Textile University, Wuhan 430200, China*

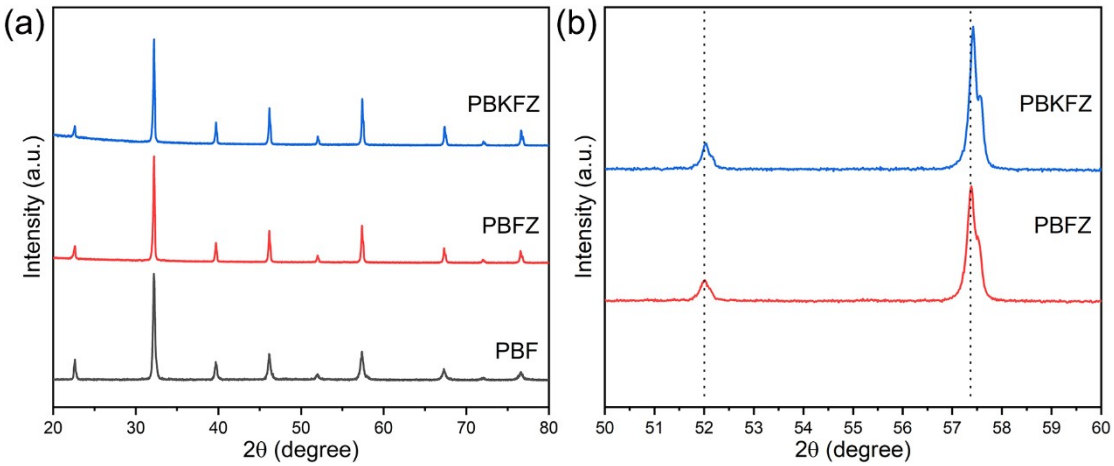


Figure S1 (a) Crystal structure of PBF, PBFZ, PBKFZ powders calcined at 1100 °C in the air for 5 h; (b) The enlargement of XRD around 50-60°.

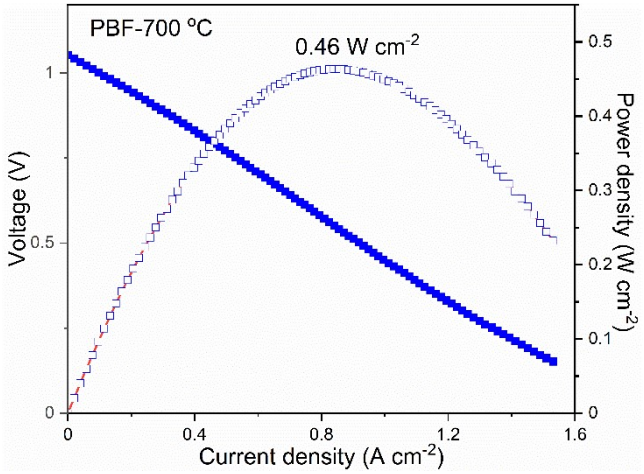


Figure S2 I-V-P curves of cells with NiO-BZCY/NiO-BZCY/BZCY/PBF single cell under 700 °C with static air as oxidant and wet hydrogen (3% $H_2O$);

Table S1 Results of Rietveld refinement for PBFZ and PBKFZ.

| **Sample** | PBFZ | PBKFZ |
|---|---|---|
| Space group | P4/mmm | P4/mmm |
| a=b (Å) | 3.93 | 3.92 |
| c (Å) | 7.87 | 7.86 |
| V (Å$^3$) | 121.85 | 121.30 |
| $\lambda^2$ | 2.15 | 3.05 |
| $R_p$ (%) | 3.95 | 4.35 |
| $R_{wp}$ (%) | 5.27 | 5.7 |

$R_p=\sum|Y_o - Y_c|/\sum Y_o$. $R_{wp}=\left[\sum w|Y_o - Y_c|^2/\sum wY_o^2\right]^{1/2}$

Table S2 The binding energy peak of $O_{ad}$, $O_L$, $Pr^{3+}$, $Pr^{4+}$, $Fe^{3+}$, $Fe^{4+}$ and the value of $O_{ad}/(O_{ad}+O_L)$, $Pr^{4+}/(Pr^{4+}+Pr^{3+})$, $Fe^{3+}/(Fe^{3+}+Fe^{4+})$ for sample.

| Sample | | PBFZ | PBKFZ |
|---|---|---|---|
| O1s | Oad | 531.33 | 531.35 |
| (eV) | $O_L$ | 528.77 | 528.72 |
| $O_{ad}/(O_{ad}+O_L)$ | | 0.62 | 0.72 |
| Pr3d5/2 (eV) | $Pr^{3+}$ | 927.97 | 927.96 |
| | | 933.78 | 933.67 |
| | $Pr^{4+}$ | 931.77 | 931.80 |
| Pr3d3/2 (eV) | $Pr^{3+}$ | 948.17 | 948.31 |
| | | 954.78 | 954.67 |
| | $Pr^{4+}$ | 952.12 | 952.20 |
| $Pr^{4+}/(Pr^{4+}+Pr^{3+})$ | | 0.46 | 0.50 |
| Fe2p3/2 | $Fe^{3+}$ | 710.25 | 710.32 |
| (eV) | $Fe^{4+}$ | 712.52 | 712.73 |
| Fe2p1/2 | $Fe^{3+}$ | 723.63 | 723.80 |
| (eV) | $Fe^{4+}$ | 723.53 | 727.32 |
| $Fe^{3+}/(Fe^{3+}+Fe^{4+})$ | | 0.69 | 0.80 |

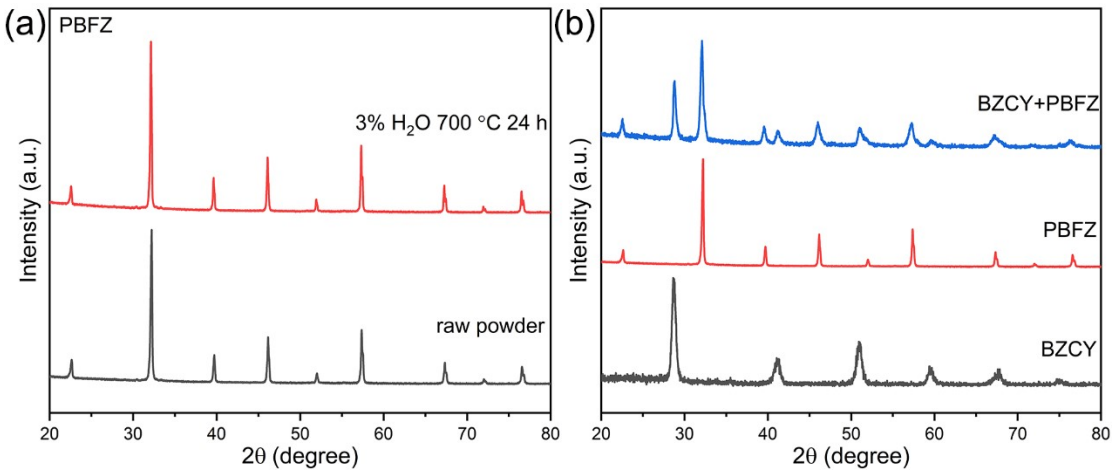


Figure S3 (a) XRD patterns for PBFZ sintered at 700 °C for 24 h under humidified air (3% $H_2O$) and (b) XRD patterns for mixed powders sintered at 900 °C for 2 h;

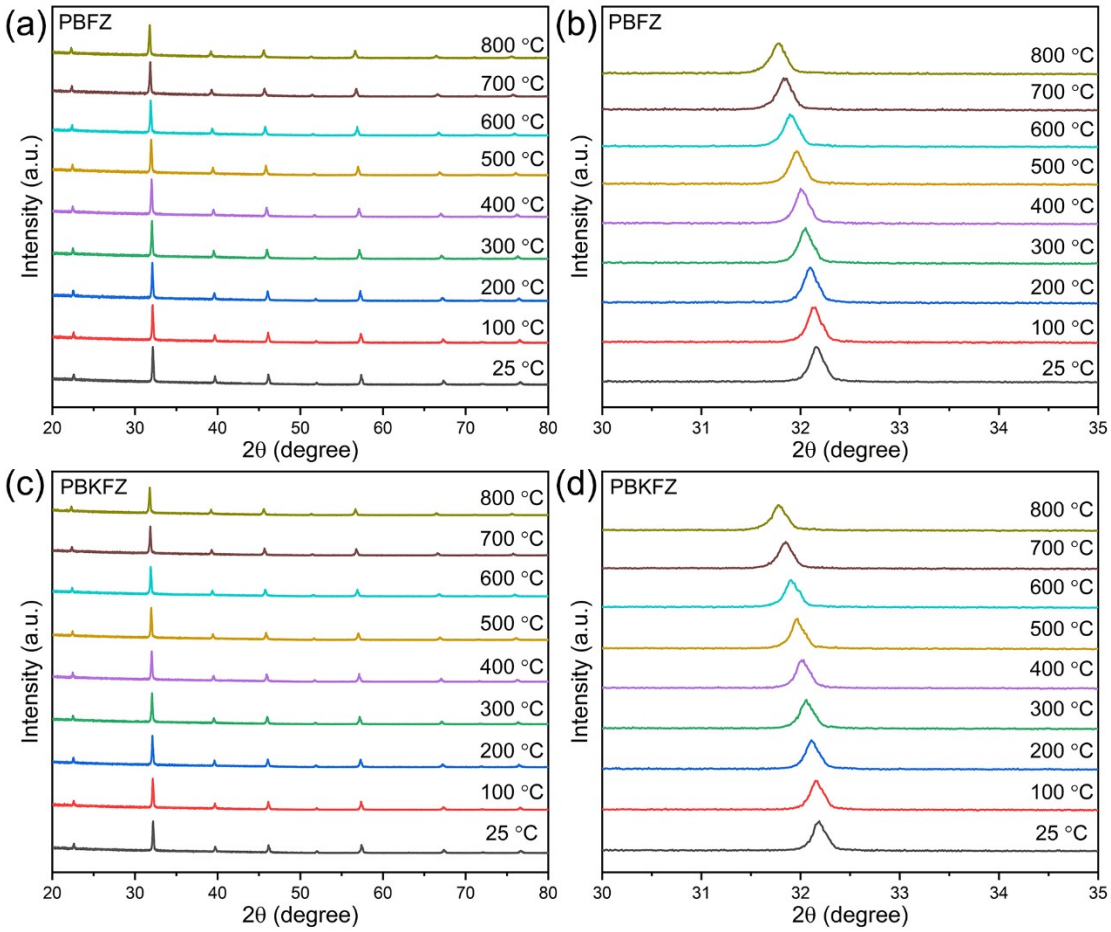


Figure S4 In situ XRD patterns of sample

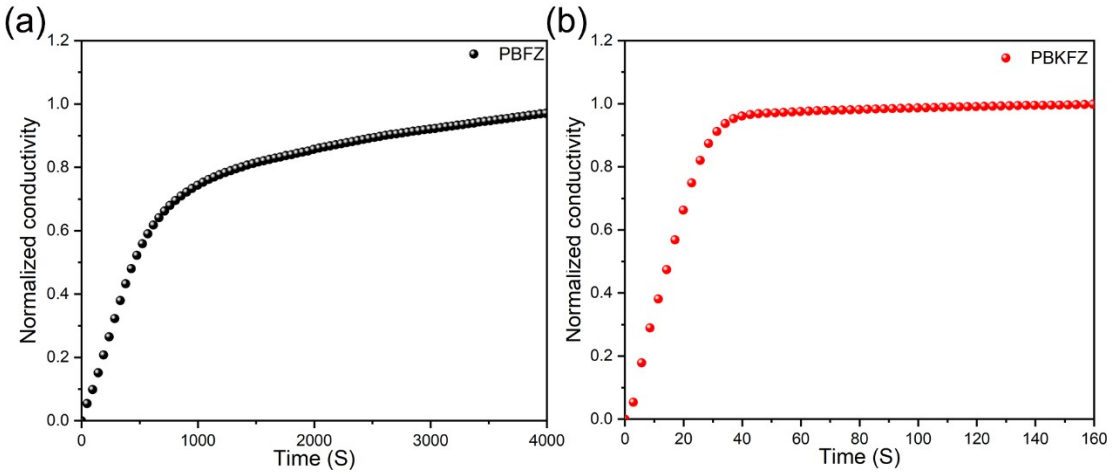


Figure S5 ECR response curves at 600 °C after a sudden change in oxygen partial pressure from 5 atm to 20 atm

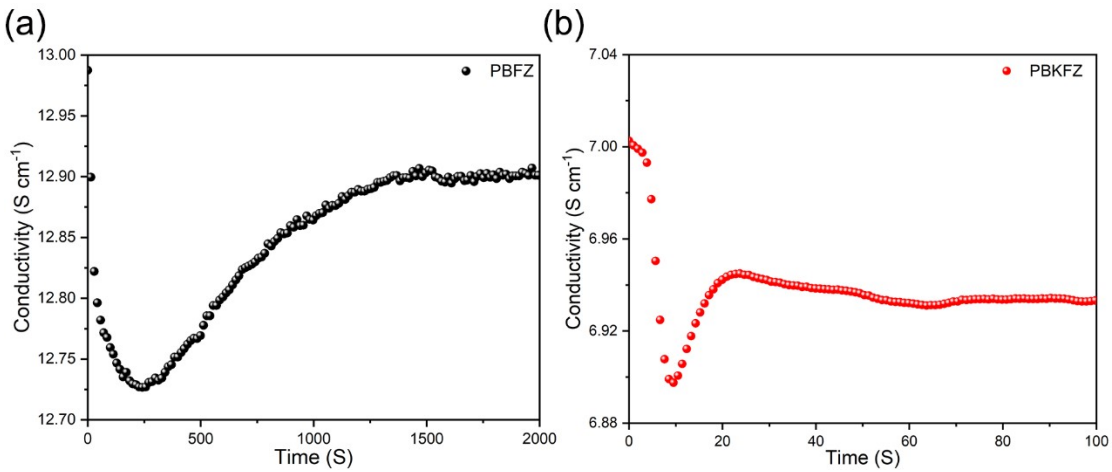


Figure S6 ECR response curves at 600 °C after a sudden change in water partial pressure from 0 atm to 3 atm

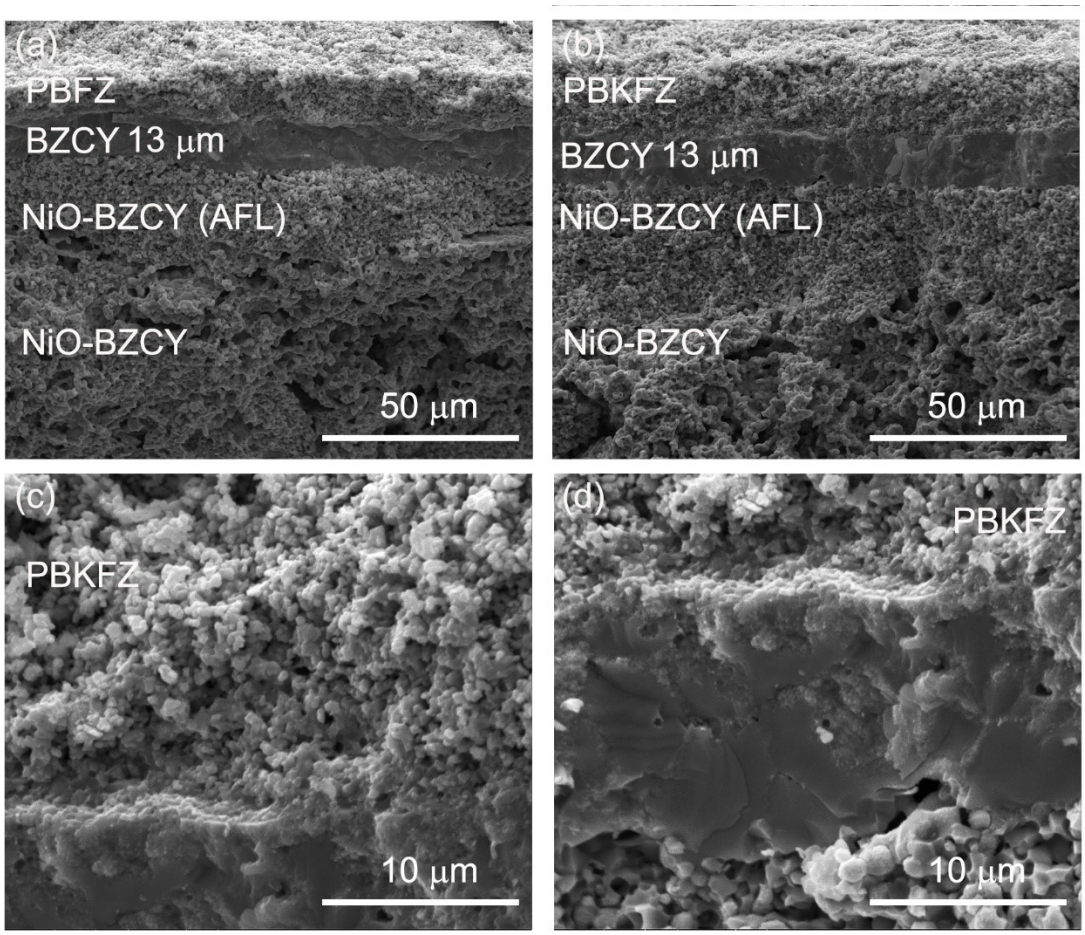


Figure S7 Cross-sectional graph of single cell: (a) NiO-BZCY/NiO-BZCY (AFL)/BZCY/PBFZ; (b) NiO-BZCY/NiO-BZCY (AFL)/BZCY/PBKFZ; (c) PBKFZ cathode structure; (d) BZCY electrolyte of PBKFZ single cell.

Table S3 Comparison of the PPD of recently reported proton-conducting fuel cells with Co-based cathode at 650 °C

| Cathode | Electrolyte (thickness, μm) | AFL | anode | PPD (W $cm^{-2}$) | Year and ref |
|---|---|---|---|---|---|
| $Ba_{0.5}Sr_{0.5}Co_{0.8}Fe_{0.2}O_{2.9-\delta}F_{0.1}$ | BCSF (10) | | NiO-BCSF | 0.37 | 2018[1] |
| $BaCo_{0.7}(Ce_{0.8}Y_{0.2})_{0.3}O_{3-\delta}$ | BZCYYb (16) | | NiO-BZCYYb | 0.98 | 2019[2] |
| $PrBaCo_2O_{5+\delta}$ | BZCY | NiO-BZCY | NiO-BZCY | 0.35 | 2009[3] |
| $NdBa_{0.5}Sr_{0.5}Co_{1.5}Fe_{0.5}O_{5+\delta}$ | BZCYYb | | NiO-BZCYYb | 1.05 | 2014[4] |
| PBSCF (without PLD layer) | BZCYYb4411 (20) | | NiO-BZCYYb4411 | 1.15 | 2018[5] |
| $Sr_2Sc_{0.1}Nb_{0.1}Co_{1.5}Fe_{0.3}O_{6-\delta}$ | BZCYYb (18.5) | | NiO-BZCYYb | 0.84 | 2019[6] |
| $BaCo_{0.4}Fe_{0.4}Zr_{0.1}Y_{0.1}O_{3-\delta}$-BCZY63 | BZCYYb | | NiO-BZCYYb | 0.45 (600 °C) | |
| $Ba_{0.5}Sr_{0.5}Co_{0.8}Fe_{0.2}O_{3-\delta}$-BZCY | BZCY (10) | NiO-BZCY | NiO-BZCY | 0.48 | 2019[7] |
| $PrBa_{0.8}Ca_{0.2}Co_2O_{5+\delta}$ exsolved $BaCoO_2$ | BZCYYb | | NiO-BZCYYb | 1.58 | 2021[8] |
| $Sm_{0.5}Sr_{0.5}CoO_{3-\delta}$ infiltrated BZY | BZY | | NiO-BZY | 0.60 (600 °C) | 2018[9] |
| PBKFZ | BZCY (13) | NiO-BZCY (20) | NiO-BZCY | 1.14 (650 °C) | This work |
| | | | | 0.74 (600 °C) | |

BCSF: $BaCe_{0.8}Sm_{0.2}F_{0.1}O_{2.85}$: BZCY: $BaCe_{0.7}Zr_{0.1}Y_{0.2}O_{3-\delta}$; BZCYYb: $BaCe_{0.7}Zr_{0.1}Y_{0.1}Yb_{0.1}O_{3-\delta}$; BZCYYb4411: $BaCe_{0.4}Zr_{0.4}Y_{0.1}Yb_{0.1}O_{3-\delta}$; BCZY63: BZCY: $BaCe_{0.7}Zr_{0.1}Y_{0.2}O_{3-\delta}$

Table S4 Comparison of the PPD of reported proton-conducting fuel cells with all reported Co-free based cathode at 650 °C

| Cathode | Electrolyte (thickness, μm) | AFL | anode | PPD (W $cm^{-2}$) | Year and ref |
|---|---|---|---|---|---|
| $Ba_{0.5}Sr_{0.5}Zn_{0.2}Fe_{0.8}O_{3-\delta}$ | BZCY (15) | | NiO-BZCY | 0.42 | 2008[10] |
| $BaCe_{0.5}Bi_{0.5}O_{3-\delta}$ | BZCY (25) | NiO-BZCY (25) | NiO-BZCY | 0.22 | 2009[11] |
| $BaCe_{0.5}Fe_{0.5}O_{3-\delta}$ | BZCY (25) | NiO-BZCY (25) | NiO-BZCY | 0.27 | 2009[12] |
| $SrFe_{0.9}Sb_{0.1}O_{3-\delta}$ | BZCYYb (25) | | NiO-BZCYYb | 0.31 | 2010[13] |
| $BaCe_{0.4}Sm_{0.2}Fe_{0.4}O_{3-\delta}$ | $BaCe_{0.8}Sm_{0.2}O_{3-\delta}$ (70) | | NiO-$BaCe_{0.8}Sm_{0.2}O_{3-\delta}$ | 0.14 | 2012[14] |
| $La_{0.6}Sr_{0.4}Fe_{0.9}Cr_{0.1}O_{3-\delta}$ | BZCY (35) | | NiO-BZCY | 0.25 | 2013[15] |
| $BaPr_{0.8}In_{0.2}O_{3-\delta}$ | BZCYYb (15) | | NiO-BZCYYb | 0.43 | 2013[16] |
| $BaCe_{0.8}Pr_{0.2}O_3$ | BZCY (25) | NiO-BZCY (15) | NiO-BZCY | 0.26 | 2014[17] |
| $La_{0.6}Sr_{0.4}Fe_{0.9}Mo_{0.1}O_{3-\delta}$ | BZCY (35) | | NiO-BZCY | 0.23 (600 °C) | 2014[18] |
| $La_{0.6}Sr_{0.4}Fe_{0.9}Nb_{0.1}O_{3-\delta}$ | BZCY (30) | | NiO-BZCY | 0.23 (600 °C) | 2014[19] |
| $La_{0.8}Sr_{0.2}MnO_3$ | $BaCe_{0.85}Y_{0.15}O_{3-\delta}$ (20) | NiO-$BaCe_{0.85}Y_{0.15}O_{3-\delta}$ (8) | NiO-$BaCe_{0.85}Y_{0.15}O_{3-\delta}$ | 0.37 | 2015[20] |
| $SrFe_{0.95}Nb_{0.05}O_{3-\delta}$ | BZCY (20) | | NiO-BZCY | 0.53 | 2017[21] |
| $LaNi_{0.6}Fe_{0.4}O_{3-\delta}$ | $BaZr_{0.8}Y_{0.2}O_{3-\delta}$ (20) | | NiO- $BaZr_{0.8}Y_{0.2}O_{3-\delta}$ | 0.10 | 2018[22] |
| Nanofiber- $LaNi_{0.6}Fe_{0.4}O_{3-\delta}$ | BZCY | | NiO-BZCY | 0.34 | 2019[23] |

Table S4. continued

| Cathode | Electrolyte (thickness, μm) | AFL | anode | PPD(W $cm^{-2}$) | Year and ref |
|---|---|---|---|---|---|
| $BaCe_{0.5}Fe_{0.3}Bi_{0.2}O_{3-\delta}$ | BZCY (20) | | NiO-BZCY | 0.67 | 2019[24] |
| $BaFe_{0.5}Sn_{0.2}Bi_{0.3}O_{3-\delta}$ | BZCY (10) | | NiO-BZCY | 1.02 | 2019[25] |
| $BaCe_{0.1}Zr_{0.2}Y_{0.1}Fe_{0.6}O_{3-\delta}$ | BZCYYb (30) | NiO-BZCYYb (23) | NiO-BZCYYb | 0.14 | 2020[26] |
| $La_{0.7}Sr_{0.3}Mn_{0.7}Ni_{0.3}O_{3-\delta}$ | BZCYYb4411 (49) | | NiO-BZCYYb4411 | 0.60 | 2020[27] |
| $BaZr_{0.2}Fe_{0.6}Y_{0.2}O_{3-\delta}$ | BZCY (20) | NiO-BZCY (20) | NiO-BZCY | 0.23 | 2020[28] |
| $BaFe_{0.8}Zn_{0.1}Bi_{0.1}O_{3-\delta}$ | BZCY (10) | | NiO-BZCY | 0.68 | 2020[29] |
| $BaCe_{0.2}Fe_{0.6}Pr_{0.2}O_{3-\delta}$ | BZCY (42) | | NiO-BZCY | 0.47 | 2021[30] |
| $La_{0.5}Sr_{0.5}Fe_{0.9}Mo_{0.1}O_{3-\delta}$ | BZCY (10) | NiO-BZCY | NiO-BZCY | 0.85 | 2021[31] |
| $PrBaCuFeO_{5+\delta}$ | BZCY (15) | | NiO-BZCY | 0.30 | 2009[32] |
| $GaBaFe_2O_{5+\delta}$ | BZCY (20) | NiO-BZCY | NiO-BZCY | 0.28 | 2010[33] |
| $PrBaFe_2O_{5+\delta}$ | BZCYYb (15) | | NiO-BZCYYb | 0.30 | 2010[34] |
| $LaBaCuFeO_{5+\delta}$ | BZCY (20) | NiO-BZCY (10) | NiO-BZCY | 0.25 | 2010[35] |
| $SmBaCuFeO_{5+\delta}$ | BZCY (20) | NiO-BZCY (10) | NiO-BZCY | 0.18 | 2010[36] |
| $GdBaFeNiO_{5+\delta}$ | BZCY (30) | | NiO-BZCY | 0.28 | 2012[37] |
| $Sr_2Fe_{1.5}Mo_{0.4}Zr_{0.1}O_{6-\delta}$ | BZCYYb (20) | | NiO-BZCYYb | 0.63 | 2020[38] |

Table S4. continued

| Cathode | Electrolyte (thickness, μm) | AFL | anode | PPD(W $cm^{-2}$) | Year and ref |
|---|---|---|---|---|---|
| $PrBaFe_2O_{5+\delta}$ | BZCY (110) | | $PrBaFe_2O_{5+\delta}$ | 0.28 | 2021[39] |
| $Pr_2NiO_{4+\delta}$ | $BaCe_{0.9}Y_{0.1}O_{3-\delta}$ (40) | | NiO-$BaCe_{0.9}Y_{0.1}O_{3-\delta}$ | 0.13 | 2009[40] |
| $Pr_2NiO_{4+\delta}$ | $BaCe_{0.55}Zr_{0.3}Y_{0.15}O_{3-\delta}$ (5) | | NiO-$BaCe_{0.55}Zr_{0.3}Y_{0.15}O_{3-\delta}$ | 0.82 | 2018[41] |
| $La_{1.2}Sr_{0.8}Ni_{0.6}Fe_{0.4}O_{4+\delta}$ | BZCY (15) | NiO-BZCY (25) | NiO-BZCY | 0.66 | 2019[42] |
| $La_{1.5}Ca_{0.5}NiO_{4+\delta}$ | BZCY (15) | | NiO-BZCY | 0.52 | 2020[43] |
| $Pr_2BaNiMnO_{7-\delta}$ | BZCYYb (12) | NiO-BZCYYb | NiO-BZCYYb | 0.76 | 2020[44] |
| $Pr_2NiO_{3.9+\delta}F_{0.1}$ | BZCYYb (20) | | NiO-BZCYYb | 0.58 | 2021[45] |
| $La_{1.6}Sr_{0.4}Cu_{0.6}Ni_{0.4}O_{4+\delta}$ | BZCYYb (15) | NiO-BZCYYb | NiO-BZCYYb | 0.50 | 2021[46] |
| $Pr_2Ni_{0.8}Cu_{0.2}O4+\delta$ | BZCYYb (26) | NiO-BZCYYb | NiO-BZCYYb | 0.28 | 2021[47] |
| $Ba_{0.5}Sr_{0.5}Zn_{0.2}Fe_{0.8}O_{3-\delta}$–$BaCe_{0.5}Zr_{0.3}Y_{0.16}Zn_{0.04}O_{3-\delta}$ | $BaCe_{0.5}Zr_{0.3}Y_{0.16}Zn_{0.04}O_{3-\delta}$ (21) | | NiO-$BaCe_{0.5}Zr_{0.3}Y_{0.16}Zn_{0.04}O_{3-\delta}$ | 0.32 | 2009[48] |
| $Ba_{0.5}Sr_{0.5}Fe_{0.8}Cu_{0.2}O_{3-\delta}$-BZCY | BZCY (20) | | NiO-BZCY | 0.30 | 2010[49] |
| $Sm_{0.5}Sr_{0.5}Fe_{0.8}Cu_{0.2}O_{3-\delta}$–$Ce_{0.8}Sm_{0.2}O_{2-\delta}$ | BZCYYb (5) | NiO-BZCYYb (15) | NiO-BZCYYb | 0.40 | 2011[50] |

Table S4. continued

| Cathode | Electrolyte (thickness, μm) | AFL | anode | PPD(W $cm^{-2}$) | Year and ref |
|---|---|---|---|---|---|
| $La_{0.7}Sr_{0.3}FeO_{3-\delta}$–$Ce_{0.8}Sm_{0.2}O_{2-\delta}$ | BZCY | | NiO-BZCY | 0.33 | 2011[51] |
| $Ba_{0.95}La_{0.05}FeO_{3-\delta}$ -BZCY | BZCY (15) | | NiO-BZCY | 0.24 | 2011[52] |
| $Ba_{0.5}Sr_{0.5}Fe_{0.9}Ni_{0.1}O_{3-\delta}$-$Sm_{0.2}Ce_{0.8}O_{1.9}$ | BZCY (25) | | NiO-BZCY | 0.32 | 2012[53] |
| $Sm_{0.5}Sr_{0.5}FeO_{3-\delta}$-BZCY | BZCY (20) | | NiO-BZCY | 0.26 | 2012[54] |
| $Ba_{0.5}Sr_{0.5}Fe_{0.9}Mo_{0.1}O_{3-\delta}$ -BZCY | BZCY (35) | | NiO-BZCY | 0.25 | 2012[55] |
| $La_{0.8}Sr_{0.2}MnO_3$-$Gd_{0.1}Ce_{0.9}O_{1.95}$ | BZCY (16) | NiO-BZCY (13) | NiO-BZCY | 0.33 (750 °C) | 2013[56] |
| $La_{0.8}Sr_{0.2}MnO_3$-$BaCe_{0.85}Y_{0.15}O_{3-\delta}$ | BZCY (16) | NiO-BZCY (13) | NiO-BZCY | 0.36 (750 °C) | 2013[56] |
| $La_{0.4}Pr_{0.4}Sr_{0.2}FeO_{3-\delta}$ - $Sm_{0.2}Ce_{0.8}O_{2-\delta}$ | BZCY (15) | | NiO-BZCY | 0.41 | 2014[57] |
| $Pr_{0.6}Sr_{0.4}Cu_{0.2}Fe_{0.8}O_{3-\delta}$ - $Ce_{0.8}Sm_{0.2}O_{2-\delta}$ | BZCY (20) | NiO-BZCY (20) | NiO-BZCY | 0.47 | 2015[58] |
| $Nd_{0.5}Ba_{0.5}Fe_{0.9}Ni_{0.1}O_{3-\delta}$-BZCY | BZCY (40) | | NiO-BZCY | 0.29 | 2016[59] |
| $Ba_{0.95}Ca_{0.05}Fe_{0.85}Sn_{0.05}Y_{0.1}O_{3-\delta}$ - $Sm_{0.2}Ce_{0.8}O_{1.9}$ | BZCY (20) | | NiO-BZCY | 0.81 | 2019[60] |
| $Ba_{0.95}Ca_{0.05}Fe_{0.85}Sn_{0.05}Y_{0.1}O_{2.9-\delta}F_{0.1}$ - $Sm_{0.2}Ce_{0.8}O_{1.9}$ | BZCY (18) | | NiO-BZCY | 0.88 | 2019[61] |

Table S4. continued

| Cathode | Electrolyte (thickness, μm) | AFL | anode | PPD(W $cm^{-2}$) | Year and ref |
|---|---|---|---|---|---|
| $La_{0.35}Pr_{0.15}Sr_{0.5}FeO_{3-\delta}$ -BZCY | BZCY (7) | NiO-BZCY | NiO-BZCY | 0.70 | 2019[62] |
| $Pr_{0.5}Ba_{0.25}Sr_{0.25}FeO_{3-\delta}$ - $Sm_{0.2}Ce_{0.8}O_{1.9}$ | BZCY (15) | | NiO-BZCY | 0.24 | 2020[63] |
| $La_{0.25}Pr_{0.25}Sr_{0.5}FeO_{3-\delta}$-BZCY | BZCY (10) | | NiO-BZCY | 0.62 (700 °C) | 2020[64] |
| $Ba_{0.95}La_{0.05}Fe_{0.8}Zn_{0.2}O_{3-\delta}$-BZCYYb | BZCYYb (42) | NiO-BZCYYb | NiO-BZCYYb | 0.20 | 2020[65] |
| $La_{1.85}Rb_{0.15}Ce_2O_7$-$La_{0.7}Sr_{0.3}FeO_3$ | BZCY | | NiO-BZCY | 0.55 | 2021[66] |
| $BaFe_{0.1}Ce_{0.8}Y_{0.1}O_{3-\delta}$ -BZCY | BZCY (15) | NiO-BZCY | NiO-BZCY | 0.53 | 2021[67] |
| $Sr_2Fe_{1.5}Mo_{0.5}O_{6-\delta}$-BZCY | BZCY (42) | | NiO-BZCY | 0.25 | 2014[68] |
| $NdBaFe_{1.9}Mn_{0.1}O_{5+\delta}$-BZCY | BZCY (30) | NiO-BZCY | NiO-BZCY | 0.45 (700 °C) | 2015[69] |
| $NdBaFe_{1.9}Nb_{0.1}O_{5+\delta}$-BZCY | BZCY (30) | NiO-BZCY | NiO-BZCY | 0.40 (700 °C) | 2015[70] |
| $K_{0.25}Sr_{1.75}Fe_{1.5}Mo_{0.5}O_{6-\delta}$-BZCY | BZCY (20) | | NiO-BZCY | 0.35 | 2021[71] |
| $LaNi_{0.6}Fe_{0.4}O_{3-\delta}$ -$La_2NiO_{4+\delta}$ | BZCY | | NiO-BZCY | 0.47 | 2014[72] |
| $Sr_3Fe_2O_{7-\delta}$ - $BaZr_{0.3}Ce_{0.5}Y_{0.2}O_{3-\delta}$ | $BaZr_{0.3}Ce_{0.5}Y_{0.2}O_{3-\delta}$ | | NiO- $BaZr_{0.3}Ce_{0.5}Y_{0.2}O_{3-\delta}$ | 0.58 | 2015[73] |
| $Nd_{1.95}NiO_{4+\delta}$-BZCYYb | BZCYYb (60) | | NiO-BZCYYb | 0.15 (750 °C) | 2015[74] |
| $La_2Ni_{0.9}Cu_{0.1}O_{4+\delta}$ | $BaCe_{0.5}Zr_{0.3}Dy_{0.2}O_{3-\delta}$ (35) | | NiO- $BaCe_{0.5}Zr_{0.3}Dy_{0.2}O_{3-\delta}$ | 0.25 | 2019[75] |

Table S4. continued

| Cathode | Electrolyte (thickness, μm) | AFL | anode | PPD(W $cm^{-2}$) | Year and ref |
|---|---|---|---|---|---|
| $LaSr_{0.8}Mn_{0.2}O_{3-\delta}$ infiltrated $BaZr_{0.8}Y_{0.2}O_{3-\delta}$ | $BaZr_{0.8}Y_{0.2}O_{3-\delta}$ (20) | | NiO-$BaZr_{0.8}Y_{0.2}O_{3-\delta}$ | 0.2 (600 °C) | 2017[76] |
| $(Pr_{0.9}La_{0.1})_2(Ni_{0.74}Cu_{0.21}Nb_{0.05})O_{4+\delta}$ infiltrated BZCY | BZCY (12) | | NiO-BZCY | 0.61 | 2017[77] |
| $LaNi_{0.6}Fe_{0.4}O_{3-\delta}$ infiltrated $La_2NiO_{4+\delta}$ | BZCY | | NiO-BZCY | 0.63 | 2018[78] |
| $La_{1.2}Sr_{0.8}NiO_{4-\delta}$ infiltrated $BaCe_{0.68}Zr_{0.1}Y_{0.1}Yb_{0.1}Cu_{0.02}O_{3-\delta}$ | BCZYYC (13) | NiO-BCZYYC (30) | NiO-BCZYYC | 0.81 | 2020[79] |
| PBKFZ | BZCY (13) | NiO-BZCY (20) | NiO-BZCY | 1.40 (700 °C)<br>1.14 (650 °C)<br>0.74 (600 °C) | This work |

1. Y. Xie, N. Shi, D. M. Huan, W. Z. Tan, J. F. Zhu, X. S. Zheng, H. B. Pan, R. R. Peng and C. R. Xia, *ChemSusChem*, 2018, **11**, 3423-3430.
2. Y. F. Song, Y. B. Chen, W. Wang, C. Zhou, Y. J. Zhong, G. M. Yang, W. Zhou, M. L. Liu and Z. P. Shao, *Joule*, 2019, **3**, 1-12.
3. L. Zhao, B. B. He, B. Lin, H. P. Ding, S. L. Wang, Y. H. Ling, R. R. Peng, G. Y. Meng and X. Q. Liu, *J. Power Sources*, 2009, **194**, 835–837.
4. J. Kim, S. Sengodan, G. Kwon, D. Ding, J. Shin, M. L. Liu and G. Kim, *ChemSusChem*, 2014, **7**, 2811-2815.
5. S. Choi, C. J. Kucharczyk, Y. G. Liang, X. H. Zhang, I. Takeuchi, H. I. Ji and S. M. Haile, *Nat. Energy*, 2018, **3**, 202-210.
6. C. Zhou, J. Sunarso, Y. F. Song, J. Dai, J. X. Zhang, B. B. Gu, W. Zhou and Z. Shao, *J. Mater. Chem. A*, 2019, **7**, 13265-13274.
7. X. Xu, H. Q. Wang, M. Fronzi, X. F. Wang, L. Bi and E. Traversa, *J. Mater. Chem. A*, 2019, **7**, 20624-20632.
8. Y. Zhou, E. Liu, Y. Chen, Y. Liu, L. Zhang, W. Zhang, Z. Luo, N. Kane, B. Zhao, L. Soule, Y. Niu, Y. Ding, H. Ding, D. Ding and M. Liu, *ACS Energy Letters*, 2021, DOI: 10.1021/acsenergylett.1c00432, 1511-1520.
9. L. Bi, S. P. Shafi, E. H. Da'as and E. Traversa, *Small*, 2018, **14**, 1801231.
10. H. P. Ding, B. Lin, X. Q. Liu and G. Y. Meng, *Electrochem. Commun.*, 2008, **10**, 1388-1391.
11. Z. T. Tao, L. Bi, L. T. Yan, W. P. Sun, Z. W. Zhu, R. R. Peng and W. Liu, *Electrochem. Commun.*, 2009, **11**, 688–690.
12. Z. T. Tao, L. Bi, Z. W. Zhu and W. Liu, *J. Power Sources*, 2009, **194**, 801-804.
13. Y. H. Ling, X. Z. Zhang, S. L. Wang, L. Zhao, B. Lin and X. Q. Liu, *J. Power Sources*, 2010, **195**, 7042-7045.
14. C. Zhang and H. Zhao, *J. Mater. Chem.*, 2012, **22**, 18387-18394.
15. Z. L. Ding, Z. J. Yang, D. M. Zhao, X. L. Deng and G. L. Ma, *J. Alloys Compd.*, 2013, **550**, 204-208.
16. Z. H. Wang, M. F. Liu, W. P. Sun, D. Ding, Z. Lü and M. L. Liu, *Electrochem.*

*Commun.*, 2013, **27**, 19-21.

17. Z. Tao, G. Hou, N. Xu, X. Chen and Q. Zhang, *Fuel Cells*, 2014, **14**, 135-138.
18. T. Yu, X. B. Mao and G. L. Ma, *Ceram. Int.*, 2014, **40**, 13747-13751.
19. T. Yu, X. B. Mao and G. L. Ma, *J. Alloys Compd.*, 2014, **608**, 30-34.
20. D.-K. Lim, H.-N. Im, B. Singh and S.-J. Song, *J. Electrochem. Soc.*, 2015, **162**, F547-F554.
21. R.-h. Yuan, W. He, C. X. Zhang, M. Ni and M. K. H. Leung, *Mater. Lett.*, 2017, **200**, 75-78.
22. K. Chen, H. Dai, S. He and L. Bi, *Fuel Cells*, 2018, **18**, 561-565.
23. H. Tang, Z. Jin, Y. Wu, W. Liu and L. Bi, *Electrochem. Commun.*, 2019, **100**, 108-112.
24. Y. S. Wu, J. Hou, Z. Gong, L. N. Miao, H. D. Tang and W. Liu, *J. Alloys Compd.*, 2019, **790**, 551-557.
25. Y. Xia, Z. Jin, H. Wang, Z. Gong, H. Lv, R. Peng, W. Liu and L. Bi, *J. Mater. Chem. A*, 2019, **7**, 16136-16148.
26. L. R. Tarutina, G. K. Vdovin, J. G. Lyagaeva and D. A. Medvedev, *J. Alloys Compd.*, 2020, **831**, 154895.
27. N. Wang, S. Hinokuma, T. Ina, C. Zhu, H. Habazaki and Y. Aoki, *J. Mater. Chem. A*, 2020, **8**, 11043-11055.
28. Y. J. Wu, K. Y. Li, Y. Yang, W. C. Song, Z. K. Ma, H. Chen, X. M. Ou, L. Zhao, M. Khan and Y. H. Ling, *J. Alloys Compd.*, 2020, **814**, 152220.
29. Y. Xia, X. Xu, Y. Teng, H. Lv, Z. Jin, D. Wang, R. Peng and W. Liu, *Ceram. Int.*, 2020, **46**, 25453-25459.
30. X. Zhou, N. Hou, T. Gan, L. Fan, Y. Zhang, J. Li, G. Gao, Y. Zhao and Y. Li, *J. Power Sources*, 2021, **495**, 229776.
31. X. Xu, Y. Xu, J. Ma, Y. Yin, M. Fronzi, X. Wang and L. Bi, *J. Power Sources*, 2021, **489**, 229486.
32. L. Zhao, B. B. He, Q. Nian, Z. Q. Xun, R. R. Peng, G. Y. Meng and X. Q. Liu, *J. Power Sources*, 2009, **194**, 291-294.
33. H. P. Ding and X. J. Xue, *J. Power Sources*, 2010, **195**, 4139-4142.

34. H. P. Ding and X. J. Xue, *J. Power Sources*, 2010, **195**, 7038-7041.
35. Y. H. Ling, B. Lin, L. Zhao, X. Z. Zhang, J. Yu, R. R. Peng, G. Y. Meng and X. Q. Liu, *J. Alloys Compd.*, 2010, **493**, 252-255.
36. Q. Nian, L. Zhao, B. B. He, B. Lin, R. R. Peng, G. Y. Meng and X. Q. Liu, *J. Alloys Compd.*, 2010, **492**, 291-294.
37. Z. J. Yang, Z. L. Ding, J. Xiao, H. M. Zhang, G. L. Ma and Z. F. Zhou, *J. Power Sources*, 2012, **220**, 15-19.
38. R. Z. Ren, Z. H. Wang, X. G. Meng, X. H. Wang, C. M. Xu, J. S. Qiao, W. Sun and K. N. Sun, *ACS Appl. Energy Mater.*, 2020, **3**, 4914-4922.
39. D. Kim, S. J. Son, M. Kim, H. J. Park and J. H. Joo, *J. Eur. Ceram. Soc.*, 2021, **41**, 5939-5946.
40. G. Taillades, J. Dailly, M. Taillades-Jacquin, F. Mauvy, A. Essouhmi, M. Marrony, C. Lalanne, S. Fourcade, D. J. Jones, J. C. Grenier and J. Rozière, *Fuel Cells*, 2009, **10**, 166-173.
41. H. An, D. Shin and H.-I. Ji, *Journal of the Korean Ceramic Society*, 2018, **55**, 358-363.
42. L. N. Miao, J. Hou, Z. Gong, Z. Z. Jin and W. Liu, *Int. J. Hydrogen Energy*, 2019, **44**, 7531-7537.
43. C.-Y. Gu, X.-S. Wu, J.-F. Cao, J. Hou, L.-N. Miao, Y.-P. Xia, F. Chao and W. Liu, *Int. J. Hydrogen Energy*, 2020, **45**, 23422-23432.
44. Q. Wang, J. Hou, Y. Fan, X.-a. Xi, J. Li, Y. Lu, G. Huo, L. Shao, X.-Z. Fu and J.-L. Luo, *J. Mater. Chem. A*, 2020, **8**, 7704-7712.
45. G. Li, Y. Gou, R. Ren, C. Xu, J. Qiao, W. Sun, Z. Wang and K. Sun, *J. Power Sources*, 2021, **508**, 230343.
46. J. Ma, Y. Pan, Y. Wang and Y. Chen, *J. Power Sources*, 2021, **509**, 230369.
47. A. P. Tarutin, Y. G. Lyagaeva, A. I. Vylkov, M. Y. Gorshkov, G. K. Vdovin and D. A. Medvedev, *Journal of Materials Science & Technology*, 2021, **93**, 157-168.
48. X. Y. Lu, Y. Z. Ding and Y. H. Chen, *J. Alloys Compd.*, 2009, **484**, 856-859.
49. L. Zhao, B. B. He, Y. H. ling, Z. Q. Xun, R. R. Peng, G. Y. Meng and X. Q. Liu, *Int. J. Hydrogen Energy*, 2010, **35**, 3769-3774.

50. Y. H. Ling, J. Yu, B. lin, X. Z. Zhang, L. Zhao and X. Q. Liu, *J. Power Sources*, 2011, **196**, 2631-2634.
51. W. P. Sun, S. M. Fang, L. T. Yan and W. Liu, *J. Electrochem. Soc.*, 2011, **158**, B1432-B1438.
52. L. T. Yan, H. P. Ding, Z. W. Zhu and X. J. Xue, *J. Power Sources*, 2011, **196**, 9352-9355.
53. Y. Z. Ding, Y. H. Chen, X. Y. Lu and B. Lin, *Int. J. Hydrogen Energy*, 2012, **37**, 9830-9835.
54. X. Y. Lu, Y. H. Chen, Y. Z. Ding and B. Lin, *Int. J. Hydrogen Energy*, 2012, **37**, 8630-8634.
55. Z. J. Yang, W. B. Wang, J. Xiao, H. M. Zhang, F. Zhang, G. L. Ma and Z. F. Zhou, *J. Power Sources*, 2012, **204**, 89-93.
56. K.-C. Lee, M.-B. Choi, D.-K. Lim, B. Singh and S.-J. Song, *J. Power Sources*, 2013, **232**, 224-233.
57. Y. H. Chen, Q. W. Gu, D. Tian, Y. Z. Ding, X. Y. Lu, W. L. Yu, T. T. Isimjan and B. Lin, *Int. J. Hydrogen Energy*, 2014, **39**, 13665-13670.
58. Z. Gong, J. Hou, Z. T. Wang, J. F. Cao, J. Y. Zhang and W. Liu, *Electrochim. Acta*, 2015, **178**, 60-64.
59. H. Shi, Z. Ding and G. Ma, *Fuel Cells*, 2016, **16**, 258-262.
60. J. J. Liu, J. W. Ding, L. N. Miao, Z. Gong, K. Li and W. Liu, *J. Alloys Compd.*, 2019, **786**, 163-168.
61. J. J. Liu, Z. Z. Jin, L. N. Miao, J. W. Ding, H. D. Tang, Z. Gong, R. R. Peng and W. Liu, *Int. J. Hydrogen Energy*, 2019, **44**, 11079-11087.
62. X. Xu, H. Q. Wang, J. M. Ma, W. Y. Liu, X. F. Wang, M. Fronzi and L. Bi, *J. Mater. Chem. A*, 2019, **7**, 18792-18798.
63. B. Cai, T.-F. Song, J.-R. Su, H. He and Y. Liu, *Solid State Ion.*, 2020, **353**, 115379.
64. J. Ma, Z. Tao, H. Kou, M. Fronzi and L. Bi, *Ceram. Int.*, 2020, **46**, 4000-4005.
65. Z. Wang, P. F. Lv, L. Yang, R. Guan, J. D. Jiang, F. D. Jin and T. M. He, *Ceram. Int.*, 2020, **46**, 18216-18223.
66. K. Dong, L. Miao, J. Hou and W. Liu, *J. Alloys Compd.*, 2021, **876**, 160205.

67. Z. Wei, J. Wang, X. Yu, Z. Li, Y. Zhao and J. Chai, *Int. J. Hydrogen Energy*, 2021, **46**, 23868-23878.
68. M. L. Li, M. Ni, F. Su and C. R. Xia, *J. Power Sources*, 2014, **260**, 197-204.
69. X. Mao, T. Yu and G. Ma, *J. Alloys Compd.*, 2015, **638**, 286–290.
70. X. B. Mao, W. B. Wang and G. L. Ma, *Ceram. Int.*, 2015, **41**, 10276-10280.
71. Y. Yang, N. Shi, Y. Xie, X. Li, X. Hu, K. Zhu, D. Huan, R. Peng, C. Xia and Y. Lu, *Electrochim. Acta*, 2021, **389**, 138453.
72. J. Hou, Z. W. Zhu, J. Qian and W. Liu, *J. Power Sources*, 2014, **264**, 67-75.
73. Z. Wang, W. Yang, S. Shafi, L. Bi, Z. Wang, R. Peng, C. Xia, W. Liu and Y. L. Lu, *J. Mater. Chem. A*, 2015, **3**, 8405-8412.
74. C. Y. Yang, X. X. Zhang, H. L. Zhao, Y. N. Shen, Z. H. Du and C. J. Zhang, *Int. J. Hydrogen Energy*, 2015, **40**, 2800-2807.
75. A. P. Tarutin, J. G. Lyagaeva, A. S. Farlenkov, A. I. Vylkov and D. M. Medvedev, *Ceram. Int.*, 2019, **45**, 16105-16112.
76. E. H. Da'as, L. Bi, S. Boulfrad and E. Traversa, *Science China Materials*, 2017, **61**, 57-64.
77. G. Li, H. Jin, Y. X. Cui, L. Q. Gui, B. B. He and L. Zhao, *J. Power Sources*, 2017, **341**, 192-198.
78. H. D. Tang, Z. Gong, Y. S. Wu, Z. Z. Jin and W. Liu, *Int. J. Hydrogen Energy*, 2018, **43**, 19749-19756.
79. C. Sun, S. Yang, Y. Lu, J. Wen, X. Ye and Z. Wen, *J. Power Sources*, 2020, **449**.